Kinetics Development with RSM. Part 3: Parameters based on Temperature vs. Time

Process Safety and Risk Management Practices

An ioMosaic White Paper

Date: September 9, 2024

How Do You Develop a Kinetic Model in Process Safety Office® SuperChems™?

A kinetic model is required for upset scenarios with runaway chemical reactions that are analyzed dynamically through SuperChems™. Kinetic parameters for these chemical reactions are usually determined by trial and error, one variable at a time. The simplest case requires two parameters, the pre-exponential factor and the activation energy. Even this unpretentious condition presents obstacles. When fixing the pre-exponential factor to determine the activation energy or vice-versa, one is optimized for the fixed value of the other, which most likely is not the real optimum. Neither parameter is optimized in this manner.

It is virtually impossible to optimize kinetic parameters by trial and error when two or more factors are present, so it makes sense to consider an alternative technique. One effective method is Experimental Design, a statistical technique that simultaneously identifies the optimum of all model factors under consideration. An experimental design organizes, conducts, and interprets the results for the best outcome based on the smallest number of trials.

The word trial usually refers to experiments. When developing a kinetic model, a trial represents a calculation with kinetic parameters that are part of the design. The typical experimental design works with squares, cubes, or hypercubes, depending on the number of input variables or predictors. A multi-dimensional cubic design is much better than trial and error. However, a superior experimental design technique can be applied to establish kinetic parameters. It is known as Response Surface Methodology (RSM) [1], carried out with a Central Composite Design (CCD) [2].

RSM is a collection of mathematical and statistical techniques for modeling and analyzing complex relationships between predictors (input variables) and responses (output variables).

This white paper employs the same chemical reaction of Part 2 of this series to provide the background for kinetic development with RSM: the exothermic di-tert-butyl peroxide decomposition in toluene. Part 2 of this series determined the kinetic parameters based on the conventional inferred self-heating rate vs. measured temperature approach. Part 3 will develop kinetic parameters based on all-measured temperature vs. time calorimetric output.

"We cannot effectively develop kinetic parameters for a runaway chemical reaction by trial and error."

The Temperature vs. Time Approach for Kinetic Development

Sometimes, the adiabatic calorimetry output may not include self-rates, but Process Safety Office® SuperChems™ calculates the self-rate derivatives for temperature and pressure. The temperature and pressure versus time data may look smooth, but occasionally their time derivatives are uneven, thus compromising kinetic development.

An alternative is to use kinetic parameters based on measured temperature versus time obtained from the experimental output instead of inferred or calculated self-heating rates. This approach requires a spreadsheet to perform calculations and Process Safety Office® SuperChems™ to test the model quality. Figure 1 summarizes the inputs necessary for both methodologies, (a) inferred data as in self-heating rate vs. temperature, which is the Part 2 of this RSM white paper series, and (b) measured data as in temperature vs. time.

Figure 1: Inputs for kinetic development. a: The conventional self-heating rate vs. temperature method; b: The alternative temperature vs. time approach

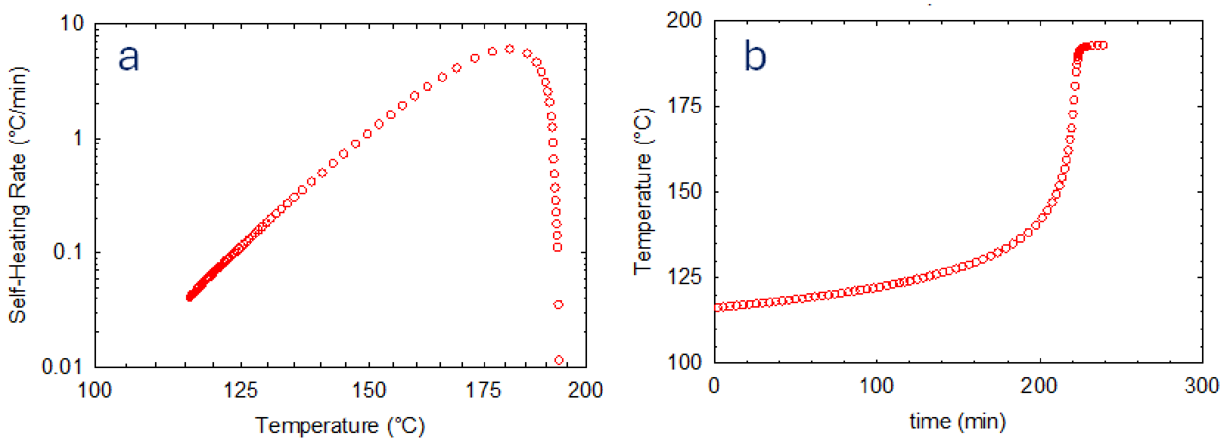

The kinetic development based on temperature vs. time starts with a simple reactant consumption rate:

$$-\frac{dC_p}{dt}=k'C_p^n \tag{1}$$

Equation (1) can be set in terms of conversion:

$$C_p=C_{po}\left(1-X\right) \tag{2}$$

from which

$$-C_{po}\frac{d\left(1-X\right)}{dt}=k'C_{po}^{n}\left(1-X\right)^{n} \tag{3}$$

or

$$-\frac{d\left(1-X\right)}{dt}=k'C_{po}^{n-1}\left(1-X\right)^{n} \tag{4}$$

and

$$1-X=\frac{T_f-T}{\Delta T_a};\ T_o<T<T_f \tag{5}$$

Combining Equations (4) and (5):

$$\frac{-1}{\Delta T_a}\frac{d\left(T_f-T\right)}{dt}=kC_{po}^{n-1}\left(\frac{T_f-T}{\Delta T_a}\right)^{n} \tag{6}$$

or

$$\frac{dT}{dt}=k\left(\frac{C_{po}}{\Delta T_a}\right)^{n-1}\left(T_f-T\right)^{n} \tag{7}$$

or

$$\frac{dT}{dt}=k\left(T_f-T\right)^{n};\ k'\left(\frac{C_{po}}{\Delta T_a}\right)^{n-1}=k=k_o e^{-\frac{B}{T}} \tag{8}$$

or

$$\frac{dT}{dt}=k_o\left(T_f-T\right)^{n}e^{-\frac{B}{T}};\ T\left(0\right)=T_o \tag{9}$$

For a first-order reaction, k = k' and therefore $k_o = k_o'$. For other reaction orders, it is necessary to apply Equation (10).

$$k = k'\left(\frac{C_{po}}{\Delta T_a}\right)^{n-1} \tag{10}$$

The temperature vs. time method requires Equation (9) to be solved. The solution is of the type t = *f*(T) as the variables are separated:

$$k_o dt = \frac{dT}{\left[T_f - T(t)\right]^n \exp\left[-\frac{B}{T(t)}\right]} \tag{11}$$

Equation (11) can be rewritten as follows:

$$k_o dt = \left[T_f - T(t)\right]^{-n} \exp\left[\frac{B}{T(t)}\right] dT \tag{12}$$

Each side of Equation (12) can be integrated:

$$k_o t + c = \int e^{\frac{B}{T(t)}} \left[T_f - T(t)\right]^{-n} dT \tag{13}$$

Zero-Order Reaction

The integration of Equation (13) is quite challenging. It is best to start with zero-order kinetics, and then build it into higher-order kinetics. For zero-order reaction, n = 0.

$$k_o t + c = \int e^{\frac{B}{T(t)}} dT \tag{14}$$

A change in variable is helpful:

$$\theta = \frac{1}{T(t)} \tag{15}$$

Equation (14) can be rewritten as follows, based on Equation (15):

$$k_o t + c = \int e^{B\theta} d\left(\frac{1}{\theta}\right) = -\int \frac{1}{\theta^2} e^{B\theta} d\theta \tag{16}$$

Integrating by parts, $\int u dv = uv - \int v du$:

$$k_o t + c = -\frac{e^{B\theta}}{\theta} - B\int \frac{e^{B\theta}}{\theta} d\theta = T(t) e^{\frac{B}{T(t)}} - B\,Ei\left[\frac{B}{T(t)}\right] \tag{17}$$

Where Ei(x) is the exponential integral function, given by Equation (18).

$$Ei(x) = -\int_{-x}^{\infty} \frac{e^{-\xi}}{\xi} d\xi \tag{18}$$

The integration constant c must be determined. At t = 0,

$$c = T_o e^{\frac{B}{T_o}} - B\,Ei\left(\frac{B}{T_o}\right) \tag{19}$$

Introduce Equation (19) into Equation (17):

$$k_o t + T_o e^{\frac{B}{T_o}} - B\,Ei\left(\frac{B}{T_o}\right) = T(t) e^{\frac{B}{T(t)}} - B\,Ei\left[\frac{B}{T(t)}\right] \tag{20}$$

Equation (20) can be manipulated to yield the relationship between the time t and the temperature T for a zero-order reaction:

$$t = \frac{1}{k_o}\left\{\left[T(t) e^{\frac{B}{T(t)}} - T_o e^{\frac{B}{T_o}}\right] - B\left\{Ei\left[\frac{B}{T(t)}\right] - Ei\left(\frac{B}{T_o}\right)\right\}\right\}; T(t) \le T_f \tag{21}$$

The knowledge gained with the development of Equation (21) can be applied to higher-order kinetics.

First-Order Reaction

For a first-order reaction, n = 1, and Equation (13) becomes:

$$k_o t + c = \int e^{\frac{B}{T(t)}} \left[T_f - T(t)\right]^{-1} dT \tag{22}$$

The change of variable is different from the one for the zero-order reaction:

$$\theta = \frac{1}{T\left(t\right)} - \frac{1}{T_f} \text{ or } T\left(t\right) = \frac{T_f}{\theta T_f + 1} \tag{23}$$

Therefore,

$$T\left(t\right) - T_f = \frac{T_f}{\theta T_f + 1} - T_f = \frac{T_f - T_f\left(\theta T_f + 1\right)}{\theta T_f + 1} = \frac{\theta T_f^2}{\theta T_f + 1} \tag{24}$$

Equation (24) is introduced into Equation (22):

$$k_o t + c = \int e^{B\theta + \frac{B}{T_f}} \frac{\theta T_f + 1}{\theta T_f^2} d\left[\frac{T_f}{\theta T_f + 1}\right] = -\int e^{B\theta + \frac{B}{T_f}} \frac{\theta T_f + 1}{\theta T_f^2} \frac{T_f^2}{\left(\theta T_f + 1\right)^2} d\theta \tag{25}$$

Equation (25) can be simplified:

$$k_o t + c = -\int e^{B\theta + \frac{B}{T_f}} \frac{1}{\theta\left(\theta T_f + 1\right)} d\theta \tag{26}$$

The integral in Equation (26) is solved by partial fraction decomposition:

$$\begin{aligned}
&-\int e^{B\theta + \frac{B}{T_f}} \frac{1}{\theta\left(\theta T_f + 1\right)} d\theta = -e^{\frac{B}{T_f}} \int e^{B\theta} \frac{1}{\theta\left(\theta T_f + 1\right)} d\theta = -e^{\frac{B}{T_f}} \int e^{B\theta} \left(\frac{1}{\theta} - \frac{T_f}{\theta T_f + 1}\right) d\theta = \\
&-e^{\frac{B}{T_f}} \int \frac{e^{B\theta}}{\theta} d\theta + e^{\frac{B}{T_f}} T_f \int \frac{e^{B\theta}}{\theta T_f + 1} d\theta = -e^{\frac{B}{T_f}} \int \frac{e^{B\theta}}{\theta} d\theta + \int \frac{e^{B\left(\theta + \frac{1}{T_f}\right)}}{\theta + \frac{1}{T_f}} d\left(\theta + \frac{1}{T_f}\right) = \\
&e^{\frac{B}{T_f}} Ei\left(B\theta\right) - Ei\left[B\left(\theta + \frac{1}{T_f}\right)\right] = e^{\frac{B}{T_f}} Ei\left\{B\left[\frac{1}{T\left(t\right)} - \frac{1}{T_f}\right]\right\} - Ei\left\{B\left[\frac{1}{T\left(t\right)} - \frac{1}{T_f} + \frac{1}{T_f}\right]\right\} = \\
&e^{\frac{B}{T_f}} Ei\left\{B\left[\frac{1}{T\left(t\right)} - \frac{1}{T_f}\right]\right\} - Ei\left\{\frac{B}{T\left(t\right)}\right\}
\end{aligned} \tag{27}$$

Introducing the result of Equation (27) into Equation (26), there results:

$$k_o t + c = e^{\frac{B}{T_f}} Ei\left\{B\left[\frac{1}{T\left(t\right)} - \frac{1}{T_f}\right]\right\} - Ei\left[\frac{B}{T\left(t\right)}\right]; \quad T\left(0\right) = T_o \tag{28}$$

The integration constant c is determined by setting t = 0 in Equation (28):

$$c = e^{\frac{B}{T_f}} Ei\left[\frac{B}{T_o} - \frac{B}{T_f}\right] - Ei\left[\frac{B}{T_o}\right] \tag{29}$$

Equation (29) is introduced into Equation (28):

$$k_o t + e^{\frac{B}{T_f}} Ei\left[\frac{B}{T_o} - \frac{B}{T_f}\right] - Ei\left[\frac{B}{T_o}\right] = e^{\frac{B}{T_f}} Ei\left[\frac{B}{T(t)} - \frac{B}{T_f}\right] - Ei\left[\frac{B}{T(t)}\right] \tag{30}$$

Equation (31) is the relationship between the time t and the temperature T for a first-order reaction:

$$t = \frac{1}{k_o}\left\{ e^{\frac{B}{T_f}} \left\{ Ei\left[B\left(\frac{1}{T_o} - \frac{1}{T_f}\right)\right] - Ei\left\{B\left[\frac{1}{T(t)} - \frac{1}{T_f}\right]\right\}\right\} + Ei\left[\frac{B}{T(t)}\right] - Ei\left(\frac{B}{T_o}\right)\right\}; T(t) \le T_f \tag{31}$$

Second-Order Reaction

For a second-order reaction, n = 2, and Equation (13) becomes:

$$k_o t + c = \int e^{\frac{B}{T(t)}} \left[T_f - T(t)\right]^{-2} dT \tag{32}$$

Equations (23) and (24) from a first-order reaction apply to a second-order reaction. Equation (24) is introduced into Equation (32) to produce Equation (33):

$$\begin{aligned} k_o t + c &= \int e^{B\theta + \frac{B}{T_f}} \left(\frac{\theta T_f + 1}{\theta T_f^2}\right)^2 d\left[\frac{T_f}{\theta T_f + 1}\right] = -\int e^{B\theta + \frac{B}{T_f}} \frac{(\theta T_f + 1)^2}{\theta^2 T_f^4} \frac{T_f^2}{(\theta T_f + 1)^2} d\theta \\ &= -\frac{e^{\frac{B}{T_f}}}{T_f^2} \int \frac{e^{B\theta}}{\theta^2} d\theta \end{aligned} \tag{33}$$

The integral in Equation (33) for a second-order reaction is identical to the integral in Equation (16) for a zero-order reaction, but the variable transformations are different. Then,

$$
\begin{aligned}
k_o t + c &= -\frac{e^{\frac{B}{T_f}}}{T_f^2}\int \frac{e^{B\theta}}{\theta^2}\,d\theta = -\frac{e^{\frac{B}{T_f}}}{T_f^2}\left[-\frac{e^{B\theta}}{\theta} - B\int \frac{e^{B\theta}}{\theta}\,d\theta\right] = \frac{e^{\frac{B}{T_f}}}{T_f^2}\left[\frac{e^{B\theta}}{\theta} - B\,Ei\left(B\theta\right)\right] \\
&= \frac{e^{\frac{B}{T_f}}}{T_f^2}\left\{\frac{e^{B\left[\frac{1}{T(t)}-\frac{1}{T_f}\right]}}{\frac{1}{T(t)}-\frac{1}{T_f}} - B\,Ei\left\{B\left[\frac{1}{T(t)}-\frac{1}{T_f}\right]\right\}\right\} \\
&= \frac{e^{\frac{B}{T_f}}}{T_f^2}\left\{\frac{T(t)T_f e^{\frac{B}{T(t)}} e^{-\frac{B}{T_f}}}{\frac{T(t)T_f}{T(t)} - \frac{T(t)T_f}{T_f}} - B\,Ei\left\{B\left[\frac{1}{T(t)}-\frac{1}{T_f}\right]\right\}\right\}
\end{aligned}
\tag{34}
$$

or

$$
k_o t + c = \frac{1}{T_f^2}\left\{\frac{T_f T(t) e^{\frac{B}{T(t)}}}{T_f - T(t)} - B e^{\frac{B}{T_f}} Ei\left\{B\left[\frac{1}{T(t)}-\frac{1}{T_f}\right]\right\}\right\}; T(0) = T_o \tag{35}
$$

Applying Equation (35) at the initial condition for t = 0, T = T$_o$:

$$
c = \frac{1}{T_f^2}\left\{\frac{T_f T_o e^{\frac{B}{T_o}}}{T_f - T_o} - B e^{\frac{B}{T_f}} Ei\left[B\left(\frac{1}{T_o}-\frac{1}{T_f}\right)\right]\right\} \tag{36}
$$

Equation (36) is introduced into Equation (35). Finally, Equation (37) is the relationship between the time t and the temperature T for a second-order reaction:

$$
\begin{aligned}
t = \frac{1}{k_o T_f^2}&\left\{\frac{T_f T(t) e^{\frac{B}{T(t)}}}{T_f - T(t)} - \frac{T_f T_o e^{\frac{B}{T_o}}}{T_f - T_o} - B e^{\frac{B}{T_f}}\left\{Ei\left\{B\left[\frac{1}{T(t)}-\frac{1}{T_f}\right]\right\} - Ei\left[B\left(\frac{1}{T_o}-\frac{1}{T_f}\right)\right]\right\}\right\} \\
&; T(t) \le T_f
\end{aligned}
\tag{37}
$$

Reaction Kinetics Summary

Formulas for the kinetics of three reaction orders based on temperature and time are the following, valid for T(t) ≤ T$_f$:

Zero-order reaction, $[k_o] = (K)^1(s)^{-1}$, Equation (21):

$$t = \frac{1}{k_o}\left\{\left[T(t)e^{\frac{B}{T(t)}} - T_o e^{\frac{B}{T_o}}\right] - B\left\{Ei\left[\frac{B}{T(t)}\right] - Ei\left(\frac{B}{T_o}\right)\right\}\right\}$$

First-order reaction, $[k_o] = (K)^0(s)^{-1}$, Equation (31):

$$t = \frac{1}{k_o}\left\{e^{\frac{B}{T_f}}\left\{Ei\left[B\left(\frac{1}{T_o} - \frac{1}{T_f}\right)\right] - Ei\left\{B\left[\frac{1}{T(t)} - \frac{1}{T_f}\right]\right\}\right\} + Ei\left[\frac{B}{T(t)}\right] - Ei\left(\frac{B}{T_o}\right)\right\}$$

Second-order reaction, $[k_o] = (K)^{-1}(s)^{-1}$, Equation (37):

$$t = \frac{1}{k_o T_f^2}\left\{\frac{T_f T(t) e^{\frac{B}{T(t)}}}{T_f - T(t)} - \frac{T_f T_o e^{\frac{B}{T_o}}}{T_f - T_o} - B e^{\frac{B}{T_f}}\left\{Ei\left\{B\left[\frac{1}{T(t)} - \frac{1}{T_f}\right]\right\} - Ei\left[B\left(\frac{1}{T_o} - \frac{1}{T_f}\right)\right]\right\}\right\}$$

For n = 0 and n = 2, a k conversion to k’ is necessary per Equation (10). There is no need for k’ conversion when n = 1.

Equation (13) has semi-analytical solutions for integer reaction orders n. The solutions are semi-analytical because the exponential integral function Ei(x) is determined numerically. The solutions become progressively longer as n increases, while fractional reaction orders require numerical integration. Semi-analytical solutions can also be developed for integer reaction orders higher than 2. In practice, they are of little interest.

The Exponential Integral Function

The exponential integral function appears multiple times when developing chemical kinetics of runaway reactions based on temperature vs. time. Gautschi and Cahill [3] discuss the properties of Ei(x). Rather than working with integrals, it is simpler to develop expansion series for Ei(x). No single series covers the entire range of the x-argument, but two expansions do.

For smaller arguments of the exponential integral function:

$$Ei(x) \approx \gamma + \ln(x) + \sum_{m=1}^{\infty}\frac{x^m}{m\,m!} \qquad x < 25 \tag{38}$$

For larger arguments of the exponential integral function:

$$Ei(x) \approx \frac{e^x}{x}\left(1+\sum_{m=1}^{\infty}\frac{m!}{x^m}\right) \qquad x > 10 \qquad (39)$$

Tabulated Ei(x) data and Equations (38) and (39) are plotted in Figure 2.

Figure 2: Exponential Integral Function Ei(x). Tabulated data and serial expansions

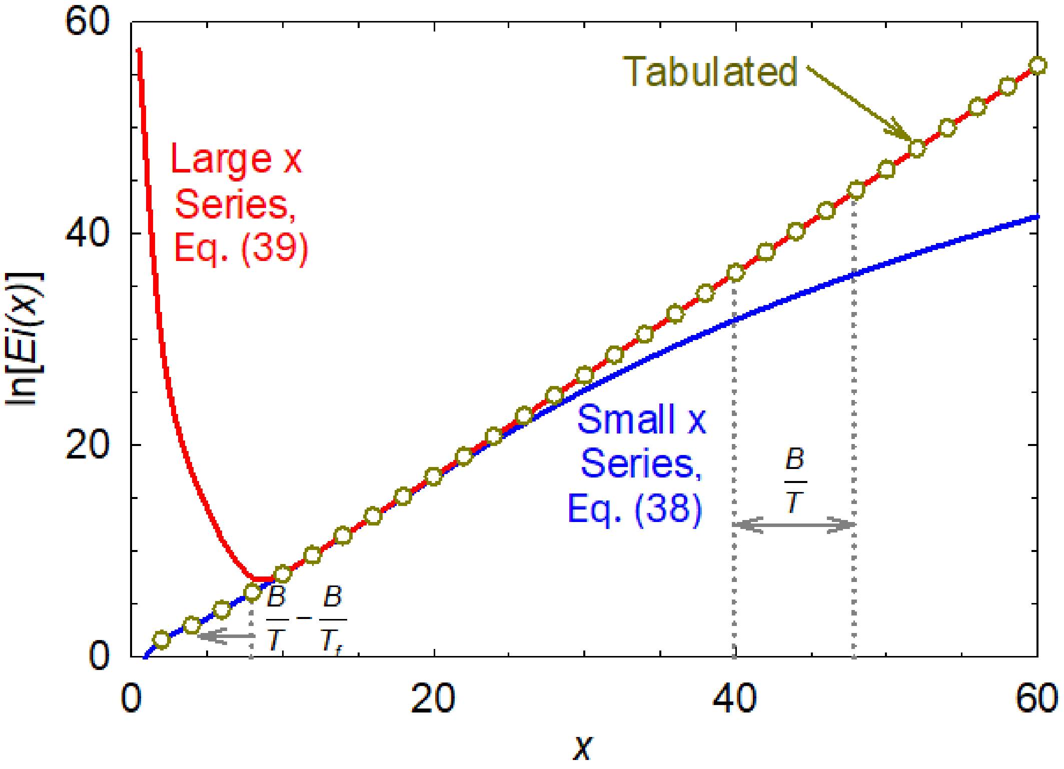

The dots represent the tabulated values obtained from the numerical integration of Equation(18). Equation (38) is a good match for Equation (18) for x smaller than 25. Equation (39) matches Equation (18) for x larger than 10. Therefore, Equations (38) and (39) overlap in the range between 10 and 25. However, the arguments are outside this range in the kinetics of runaway reactions. $B/T-B/T_f$ is typically less than 8, so Equation (38) must be used. On the other hand, B/T usually falls in the range between 40 and 48, so Equation (39) is applied.

RSM for the Decomposition of DTBP in Toluene

Response Surface Methodology [1] combines with Central Composite Design (CCD) [2] to examine the relationship between model response variables and continuous predictors or factors. The method works best when only important controllable factors are applied. RSM Part 2 of this series explored adiabatic calorimetry, stoichiometry, decomposition products, and kinetic modeling based on self-rates of DTBP decomposition in toluene. The reader is referred to that white paper before proceeding with this document.

This white paper aims to determine the values of the k_o and B model factors or parameters for the decomposition of di-tert-butyl peroxide in toluene using only measured data, or the temperature vs. time method. The decomposition of DTBP in toluene is a first-order reaction, according to RSM Part 2. This design's objective is to match key experimental outputs, and the "experiments" are Excel calculations with assigned values of the predictors. The intent of this white paper is not to teach statistics. There are publications that the reader might consult, such as Box [4], Kiemele et al.[5], Montgomery [6], and Spiegel and Stephens [7]. The knowledge of experimental design in statistics is a plus when reading this white paper.

Model parameters in statistics are essentially regression coefficients, such as k_o and B in this application. A predictor forecasts the outcome of the response variables. In this application, the predictors are temperatures, and the responses are times. The design's goal is to match simulation responses with experimentation.

The approach in this study is to use a full-factorial design, augmented by central point and star points, which account for curvature, that is, quadratic terms and two-way interactions. Two-way interactions are much more common than higher-order interactions, which rarely occur. The Central Composite Design was modified with one central point instead of the standard model with multiple central points. The reason is that the "experiments" in this evaluation are spreadsheet calculations. Contrary to actual experiments, the results are identical with any number of runs for the same values of the predictors. Minitab is the software used in this development. Other advanced statistical software can also be used.

Many predictors can be included in the design, such as pre-exponential factors, activation energies, reaction orders, binary interaction parameters, stoichiometric coefficients, and so forth. However, the design becomes increasingly complex as the number of predictors increases. For CCD with one central point, the number of spreadsheet simulations for a full factorial design is 2^k+2k+1, where k is the number of predictors. For the two predictors in this study, k_o and B, the design is based on 2^2+2x2+1 = 9 simulations. Additional points must be added if at least one of the predictors is pegged at one of the design limits.

This study can be summarized as follows:

Model parameters or factors:

- Natural logarithm of the pre-exponential factor, k_o (min^{-1})
- Activation energy divided by the universal gas constant, B (K)

Predictors or forecasting variables: Temperatures

- Below the inflection point, 140°C
- At about the inflection point, 160°C
- Above the inflection point, 180°C

Responses or outputs based on the sigmoid curve of T(t) vs. t of Figure 1b: Times

- Before the inflection point at 140°C: 206.52 min
- At about the inflection point at 160°C: 226.53 min
- After the inflection point at 180°C: 236.53 min

Figure 3 represents the values of this design’s parameters.

Figure 3: Parameters of the response surface central composite design

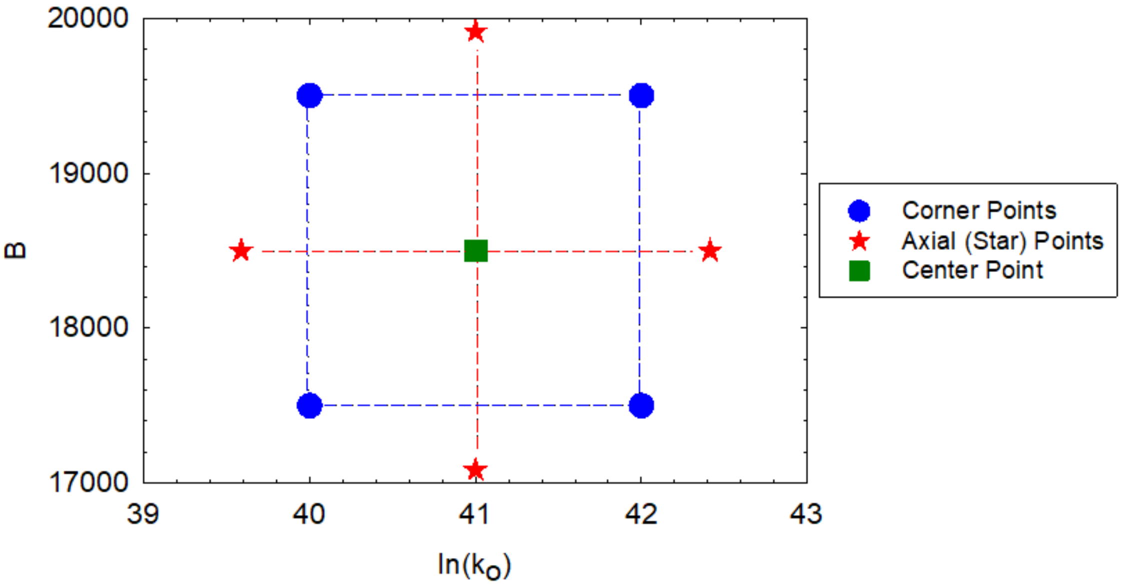

Equation (31) was applied in combination with Equations (38) and (39) to generate the results in Table 1. T_o is 115.78°C and T_f is 193.14°C, which must be converted to kelvin to be entered in Equation (31).

Table 1: Simulation outputs in Excel at the CCD points

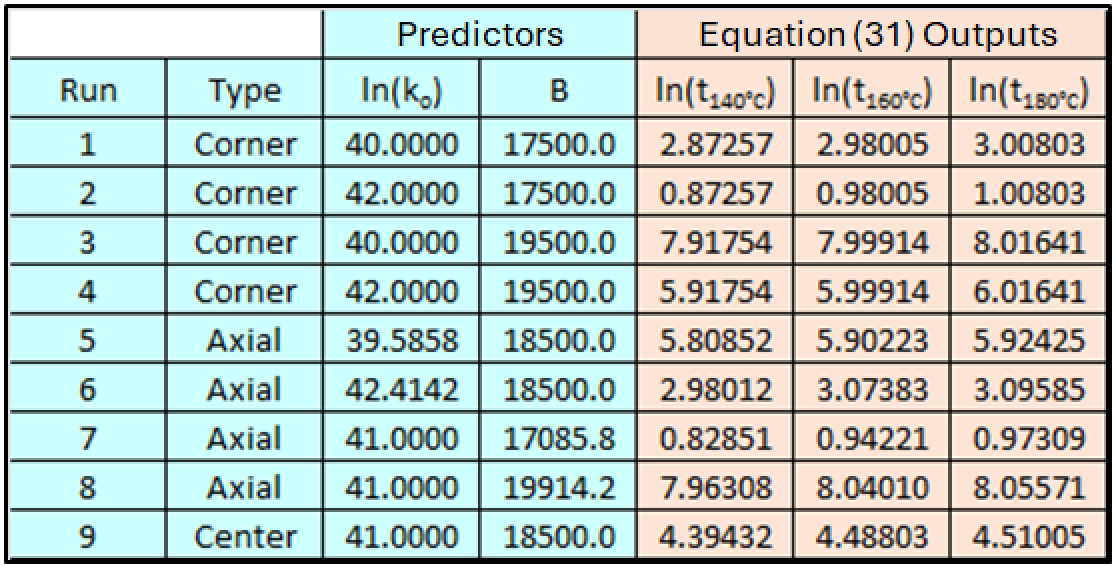

		Predictors		Equation (31) Outputs		
Run	Type	$\ln(k_o)$	B	$\ln(t_{140°C})$	$\ln(t_{160°C})$	$\ln(t_{180°C})$
1	Corner	40.0000	17500.0	2.87257	2.98005	3.00803
2	Corner	42.0000	17500.0	0.87257	0.98005	1.00803
3	Corner	40.0000	19500.0	7.91754	7.99914	8.01641
4	Corner	42.0000	19500.0	5.91754	5.99914	6.01641
5	Axial	39.5858	18500.0	5.80852	5.90223	5.92425
6	Axial	42.4142	18500.0	2.98012	3.07383	3.09585
7	Axial	41.0000	17085.8	0.82851	0.94221	0.97309
8	Axial	41.0000	19914.2	7.96308	8.04010	8.05571
9	Center	41.0000	18500.0	4.39432	4.48803	4.51005

The output of the Minitab analysis is shown in Table 2. The reduced model comes from the elimination of terms that are not statistically significant.

Table 2: Statistical output of the reduced model

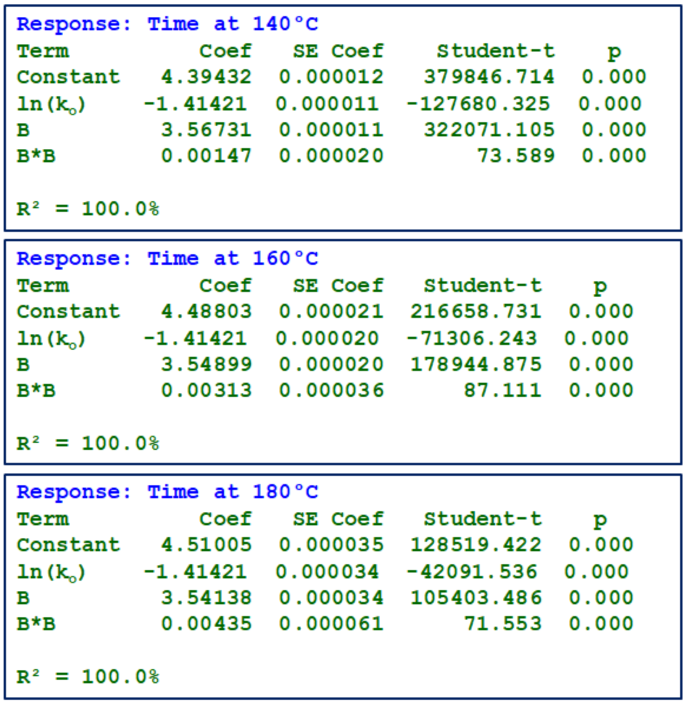

```
Response:  Time at 140°C
Term          Coef    SE Coef    Student-t     p
Constant   4.39432  0.000012   379846.714  0.000
ln(ko)    -1.41421  0.000011  -127680.325  0.000
B          3.56731  0.000011   322071.105  0.000
B*B        0.00147  0.000020       73.589  0.000

R² = 100.0%
```

```
Response:  Time at 160°C
Term          Coef    SE Coef   Student-t     p
Constant   4.48803  0.000021  216658.731  0.000
ln(ko)    -1.41421  0.000020  -71306.243  0.000
B          3.54899  0.000020  178944.875  0.000
B*B        0.00313  0.000036      87.111  0.000

R² = 100.0%
```

```
Response:  Time at 180°C
Term          Coef    SE Coef   Student-t     p
Constant   4.51005  0.000035  128519.422  0.000
ln(ko)    -1.41421  0.000034  -42091.536  0.000
B          3.54138  0.000034  105403.486  0.000
B*B        0.00435  0.000061      71.553  0.000

R² = 100.0%
```

The outputs in Table 2 are explained considering the possible model terms:

Constant	Intercept
$\ln(k_o)$	First order
B	First order
$[\ln(k_o)]^2$	Second order
B^2	Second order
$\ln(k_o)$*B	Interaction

$[\ln(k_o)]^2$ and $\ln(k_o)$*B were not statistically significant in this design. They were dropped from the reduced model, and do not appear in Table 2.

Table Headings

- Coefficients: Estimates that multiply the predictors to calculate the fitted value of the responses
- Standard Error of the Coefficients: It measures the precision of the model estimates. In other words, it is the standard deviation of the respective term.
- Student-t: Value of the student t-distribution to determine the probability p of the null hypothesis, that is, that the term is not statistically significant.

- p: Null-hypothesis test, how well the predictor and the response correlate. The null hypothesis (no effect) is typically rejected at a p-value < 0.05. Some analysts are more lenient and reject the null hypothesis for p-value < 0.1 in experimental design. A low p-value means the null hypothesis is rejected and the term is statistically significant.

An experimental design requires an optimization procedure. The optimization is done through the desirability function [8]. The higher the desirability, the better the quality of the model. Figure 4 displays this study's desirability output in a graph.

Figure 4: Desirability analysis for the factors of the DTBP decomposition design

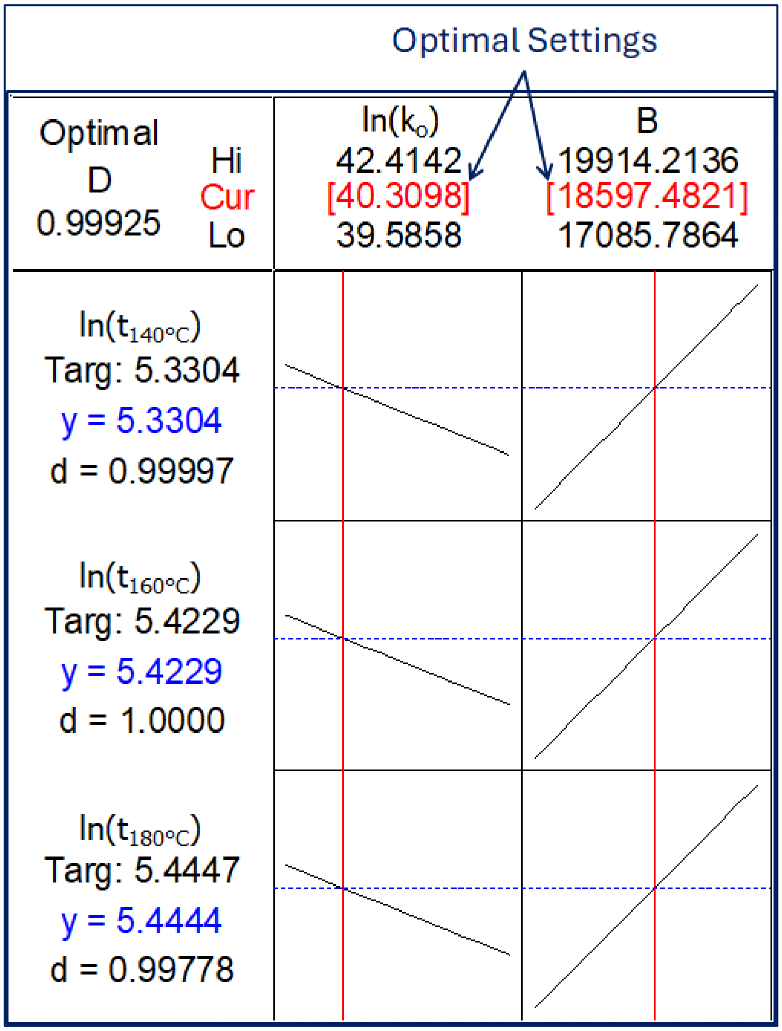

The optimal desirability D is the geometric mean of the individual desirability values d:

$$D = \sqrt[3]{d_1 d_2 d_3}$$
$$D = \sqrt[3]{(0.99997)(1.00000)(0.99778)}$$
$$D = 0.99925$$

Figure 4 indicates the calculated times (y's) are very close to the experimental data (targets), so the optimal or combined desirability is close to 1. The individual optima of the factors ln(k_o) and B are in red. The vertical red lines for the parameters are well within the limits of the design, that is, they are not pegged at one end, which would require rework.

Figure 5 shows the graph in Figure 3 plus the optimum conditions of ln(k_o) and B, highlighted in red in Figure 4. The optimum is well within the limits of the design.

Figure 5: Parameters of the response surface central composite design with the optimum point

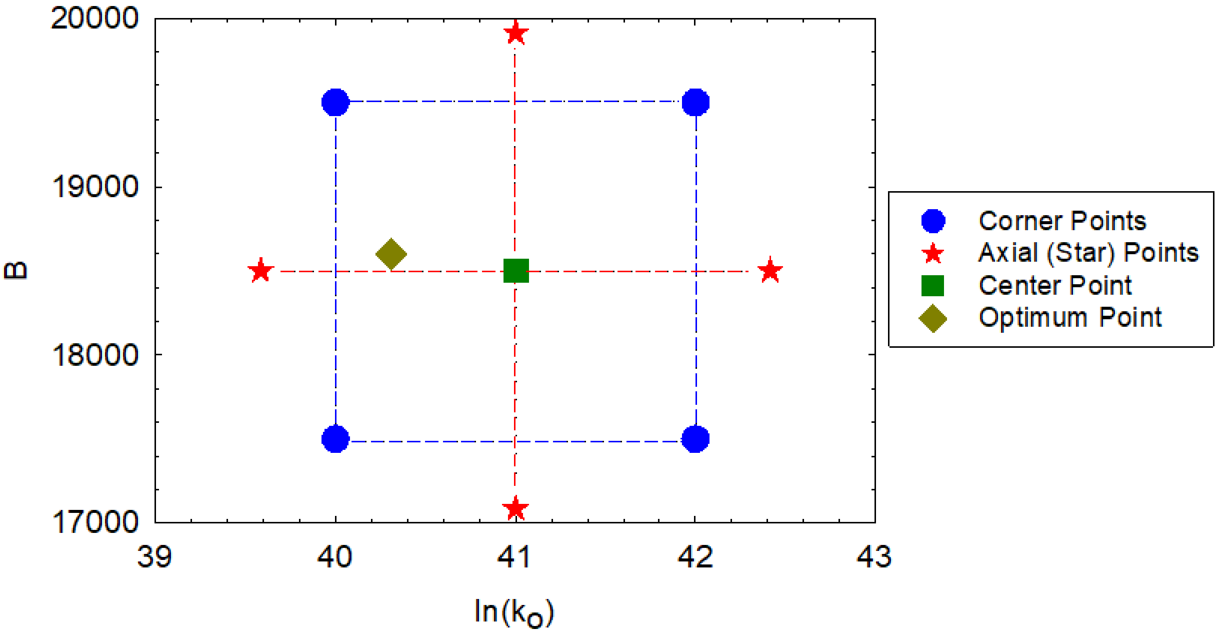

Figure 6 shows an overlaid contour plot for the two parameters, ln(k_o) and B, and a white zone, the intersection of the three bands, where the three design responses reach their targets. The design's optimum is within the white zone, as required.

Figure 6: Overlaid contour plot for the design

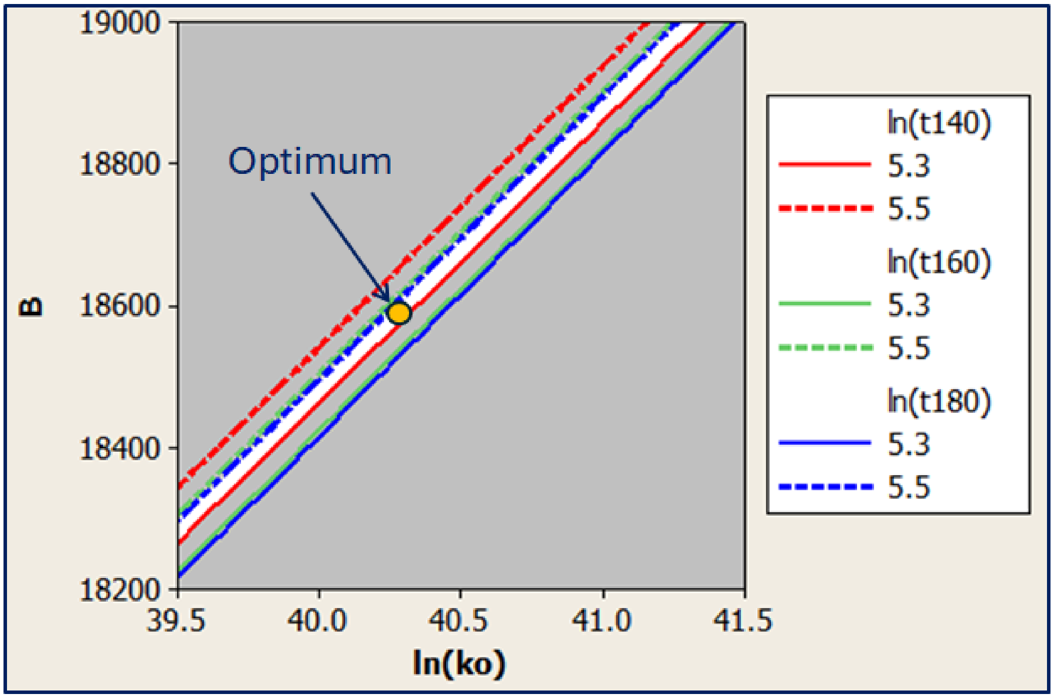

Figure 7 includes three outputs. The light brown circles symbolize the experimental data. The blue line represents the curve calculated with Equation (31) with the optimized parameters of Figure 4. The pink squares are the three design responses of time that correspond to the temperatures of 140, 160, and 180°C. As can be seen in Figure 7, the three data sources coincide with one another. Response Surface Methodology in Figure 4 correctly identifies the optimum kinetic parameters k_o and B.

Figure 7: Temperature vs. time for di-tert-butyl peroxide decomposition in toluene

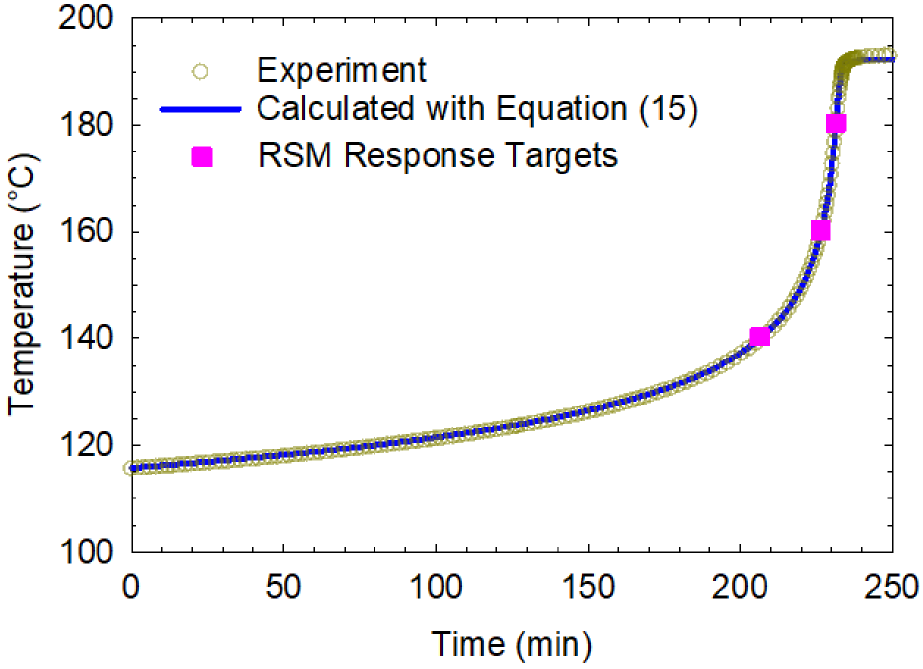

Comparison of T vs. t with dT/dt vs. T

The second white paper of the RSM series covered the determination of kinetic parameters for the DTBP decomposition in toluene based on self-heating rate vs. temperature. dT/dt vs. T and T vs. t use the same statistical methodology and statistics program, with different software that generates model responses, as seen in Table 3.

Table 3: Software to develop kinetic parameters for DTBP decomposition in toluene

Method	SuperChems™	Excel	Minitab*
RSM $\frac{dT}{dt}\ vs.T$	✓		✓
RSM $T\ vs.t$		✓	✓

* Or other quality statistics software

The predictors of the *RSM dT/dt vs. T* method were entered in Process Safety Office® SuperChems™ to generate responses by dynamic simulations. The *predictors of the T vs. t* approach were inserted in Excel to calculate responses through Equation (31). The optimized parameters for both methods are shown in Table 4.

Table 4: Optimized kinetic parameters for DTBP decomposition in toluene

Method	**k_o (s^{-1}) ***	**B**
RSM $\frac{dT}{dt}$ vs. T	6.6961×10^{15}	18695
RSM T vs. t	5.3477×10^{15}	18597

* Converted from min^{-1} to s^{-1} for introduction in Process Safety Office® SuperChems™

Even though the responses in both methods were calculated using very different techniques, the optimal values of k_o and B are very similar. Indeed, no visual differences can be discerned in a graph when k_o*exp(-B/T) vs. T is plotted for both methods, but they can be quantified in Table 5.

Table 5: Process Safety Office® SuperChems™ simulation comparisons

Method	$\left(\frac{dT}{dt}\right)_{154°C}$	$\left(\frac{dT}{dt}\right)_{max}$	t_r
Experimental	**1.57081**	**6.04968**	**221.70**
RSM $\frac{dT}{dt}$ vs. T	**1.55809**	**6.05534**	**221.99**
RSM T vs. t	**1.56576**	**6.00147**	**220.33**
Deviation	**%**	**%**	**%**
RSM $\frac{dT}{dt}$ vs. T	**-0.810**	**0.094**	**0.131**
RSM T vs. t	**-0.321**	**-0.797**	**-0.618**

Notes:

- 154°C is the mid-point temperature of the experiment and simulations.
- The maximum temperature is 193.14°C.
- t_r is the time to the maximum rate.

- dT/dt is obtained by Process Safety Office® SuperChems™ simulations.

In perspective, chemical kinetics parameters developed with measured or inferred data in combination with Response Surface Methodology compare very well with the experimental data for di-tert-butyl peroxide decomposition in toluene.

Once the optimal settings for both methods are determined, simulations can be carried out in Process Safety Office® SuperChems™ to check their quality in temperature vs. time and self-heating rate vs. temperature plots.

Figure 8 shows dynamic simulation graphs of temperature vs. time obtained with kinetic parameters developed by the T vs. t and dT/dt vs. T methods. As can be seen, the outputs are indistinguishable.

Figure 8: Time vs. temperature for di-tert-butyl peroxide decomposition in toluene

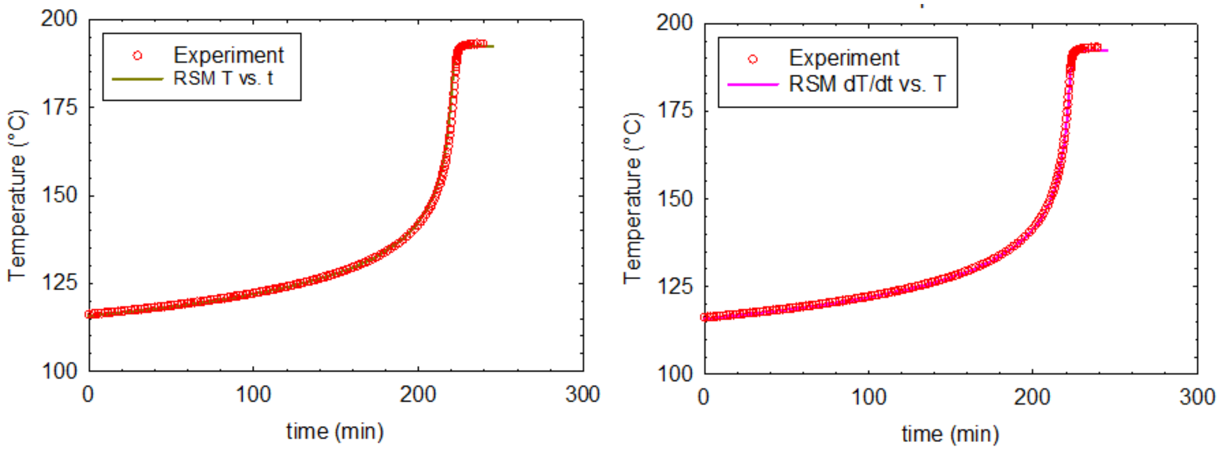

Figure 9 displays graphs on self-heating rate vs. temperature for the two methods. As in Figure 8, the results are virtually identical.

Figure 9: Self-heating rate vs. temperature for di-tert-butyl peroxide decomposition in toluene

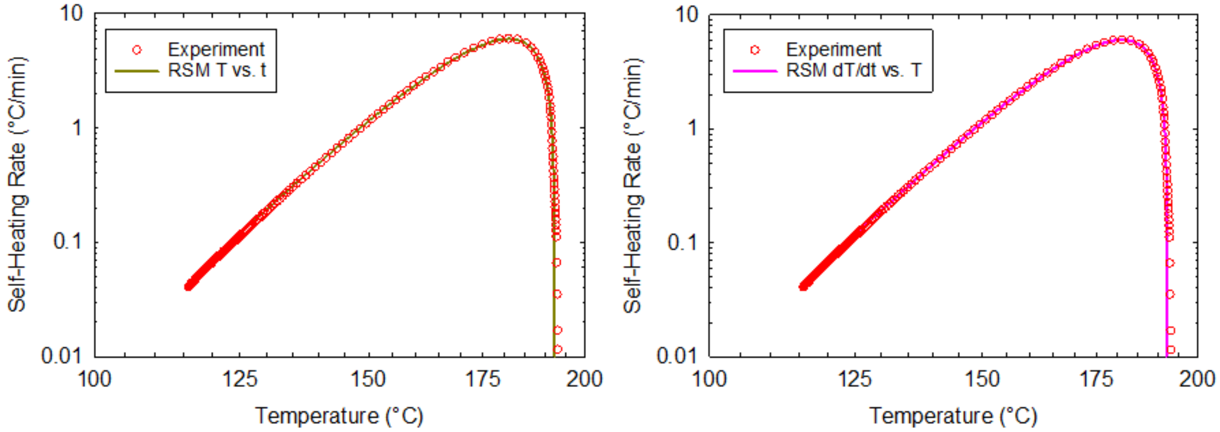

The curves in Figure 9 can be further examined by focusing on two zones: at the beginning and the peak of the runaway reaction. Figure 10 validates the two methods at the beginning of reactivity, while Figure 11 focuses on maximum rates.

Figure 10: Reactivity onset – self-heating rate vs. temperature for di-tert-butyl peroxide decomposition in toluene

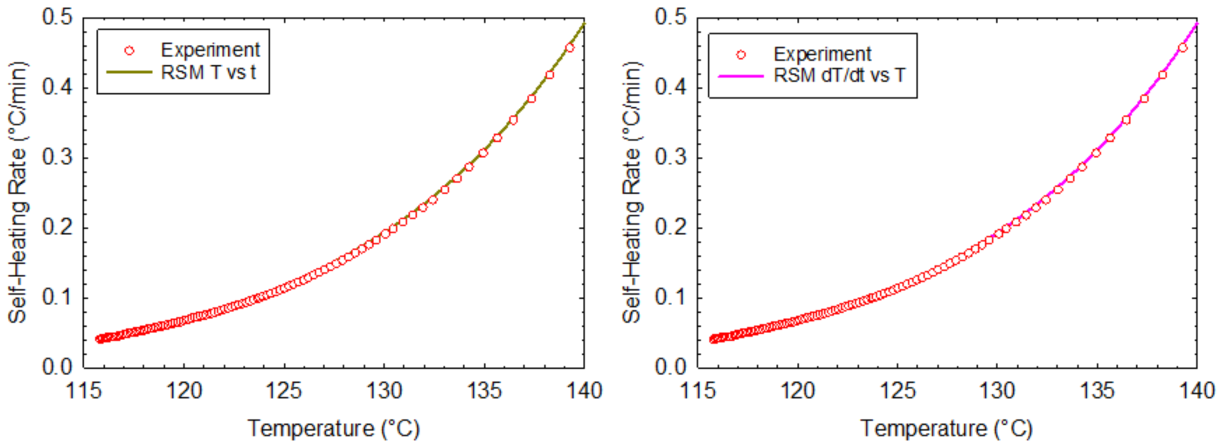

Figure 11: Peak reactivity – self-heating rate vs. temperature for di-tert-butyl peroxide decomposition in toluene

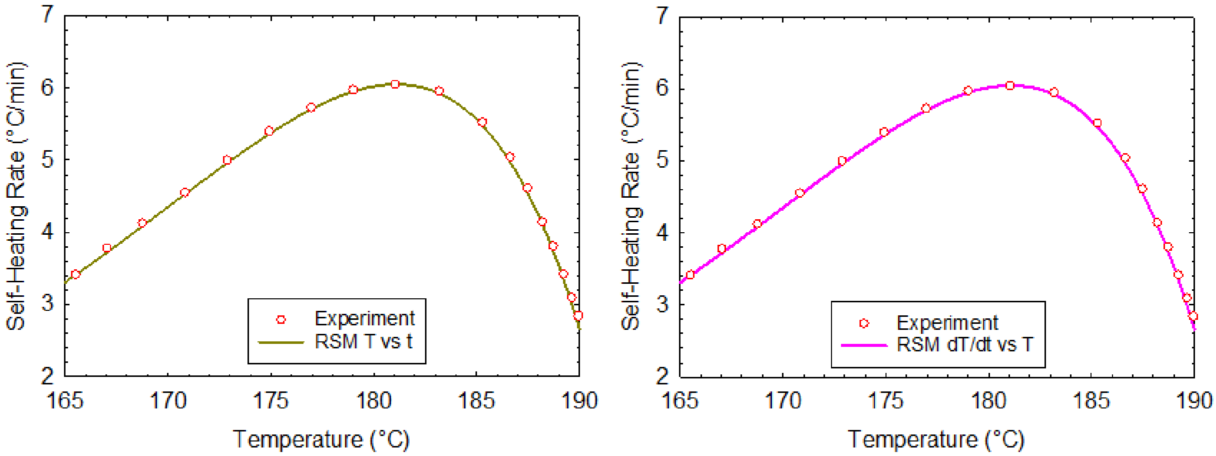

Conclusions

An experimental design was performed in this white paper for di-tert-butyl peroxide decomposition in toluene employing observed temperature vs. time data. The model's foundation is based on developing a material balance for DTBP decomposition, setting the concentration as a function of temperature, separating the variables T and t, and then integrating both sides of the equation. The solution is semi-analytical because it contains the exponential integral function, which must be determined numerically.

The results were compared with the experimental design based on inferred self-heating rate vs. temperature data, the most common approach, covered in the second white paper of this series.

The experimental design with direct measurements considered an advanced statistics software that optimizes multiple parameters simultaneously, based on data generated in a sealed adiabatic calorimeter. The statistical method is Response Surface Methodology (RSM) with a Central Composite Design, which estimates first and second-order terms. The "experiments" of the temperature vs. time design were Excel spreadsheet calculations with the integrated T vs. t equation for a first-order reaction.

It is virtually impossible to optimize multiple parameters concurrently by trial and error. RSM is an approach that optimizes two or more predictors together. T vs. t and dT/dt vs. T analyses produced almost indistinguishable kinetic parameters for this system. The outcome of dynamic simulations with either set of kinetic parameters are virtually identical.

This white paper demonstrates that an experimental design can establish kinetic parameters directly from measured data.

Author

1. Enio Kumpinsky; kumpinsky.e.nh@ioMosaic.com

Figure Sources

Figures 1-3, 5, 7-11: SigmaPlot® Scientific Graphing and Statistics Software

Figures 4, 6: Minitab® Statistics Software

Nomenclature

c	Integration constant
C	Molar concentration
C_p	Molar concentration of di-tert-butyl peroxide (DTBP)
C_{po}	Initial molar concentration of di-tert-butyl peroxide
DTBP	Di-Tert-Butyl Peroxide
k’	Kinetic rate constant for simulations
k_o’	Pre-exponential factor for the kinetic rate constant
k	Lumped kinetic rate constant
k_o	Pre-exponential factor, lumped kinetics, calorimetry
B	Activation energy divided by the universal gas constant
n	Reaction order
t	Time
T	Temperature
T_o	Onset temperature of the runaway reaction
T_f	Final temperature of runaway reaction
X	Conversion of di-tert-butyl peroxide
ΔT_a	Adiabatic temperature rise, $T_f - T_o$
θ	Transformation 1/T for a zero-order reaction and $1/T-1/T_f$ for a first-order reaction
ξ	Variable of the exponential integral function Ei(x)

Additional ioMosaic White Paper Resources

It is impossible to cover all aspects and facets of chemical reactivity management in one white paper. The resources provided below address in more detail several key topics and can be requested from sales@iomosaic.com or melhem@iomosaic.com:

Chemical Reactivity Management

1. Systematic Evaluation of Chemical Reaction Hazards
2. Quickly Develop Chemical Interaction Matrices with SuperChems
3. Thermal Stability Indicators
4. Calculate Phase and Chemical Equilibria Using Process Safety Office SuperChems Expert
5. An Advanced Method for the Estimation of Reaction Stoichiometry and Rates from ARC Data
6. Development of Kinetic Models - Part I. Thermal Stability
7. Development of Kinetic Models - Part II. Pressure Relief Systems
8. Forget direct scaleup vent sizing and master kinetic modeling instead
9. Polymerization Modeling for Emergency Relief Systems
10. Polymerization Reactions Inhibitor Modeling - Styrene and Butyl Acrylate Incidents Case Studies
11. Polymerization Models for butadiene, vinyl acetate, acrylates, acrylonitrile, and isoprene

Fire Modeling

2. Fire Exposure Modeling Considerations
3. RAGAGEP Considerations for Overtemperature Protection in Relief Systems

Pressure Relief and Vent Containment Design

1. Two-phase Flow Onset and Disengagement Methods
2. Vent Containment Design For Emergency Relief Systems
3. Forget the Omega Method and Master vdP Integration Instead
4. Advanced Pressure Relief Design Using Computer Simulation
5. Beware of Temperature Increase During Rapid Vessel Charging
6. Heat of vaporization considerations for relief systems applications
7. Properly Calculate Relief Systems Reaction Forces

8. Realize Better Risk Characterization of STHE Tube Failure Scenarios Through Relief Systems Dynamics Modeling
9. Relief and Flare Systems Statics vs Dynamics
10. Relief Requirements for Distillation Columns
11. Retrograde and Phase Change (RPC) Flow Considerations for Relief and Depressuring Systems
12. Retrograde and Phase Change (RPC) Flow Considerations for Relief and Flare Systems
13. Single and Multiphase Control Valve Flow
14. The Anatomy of Liquid Displacement and High-Pressure Fluid Breakthrough
15. Thermal Expansion Relief Requirements for Liquids, Vapors, and Supercritical Fluids
16. Quantify Non-Equilibrium Flow and Rapid Phase Transitions

PRV Stability

1. Analysis of PRV Stability In Relief Systems - Detailed Dynamics - Part I
2. Analysis of PRV Stability In Relief Systems - Screening - Part II
3. Analysis of PRV Stability In Relief Systems - How to Avoid the Singing PRV Problem - Part III
4. Analysis of PRV Stability In Relief Systems - On the Estimation of Speed of Sound - Part IV
5. Analysis of PRV Stability In Relief Systems - Get a Handle on PRV Stability - Part V
6. PRV stability inlet line critical length
7. PRV Stability - Bridging the 3 percent pressure loss rule gap

Fire and Explosion Modeling

1. Calculate Flammability Limits Using Process Safety Office ®SuperChems Expert
2. How Flame Arresters Work
3. Development of Reduced Analytical Models for Explosion Dynamics
4. Quantify Explosion Venting Dynamics in Vessels Enclosures and Energy Storage Systems

Process Safety Management and Automation

1. Effectively Manage Mechanical Integrity in Process Safety Enterprise®
2. Effectively Manage Changes to Processes, Chemicals, Equipment, and Personnel Using Process Safety Enterprise®
3. Properly Evaluate Building and Facility Siting Risks
4. Emergency Response and Process Hazard Analysis Charts
5. Usage of AEGL Dosage in Safety and Risk Studies
6. Driving Safety and Business Performance Through Data Mining

References

[1] Response Surface Designs. NIST Engineering Statistics Handbook, 5.3.3.6, National Institute of Standards and Technology at the U.S. Department of Commerce.

[2] Central Composite Design. NIST Engineering Statistics Handbook, 5.3.3.6.1, National Institute of Standards and Technology at the U.S. Department of Commerce.

[3] W. Gautschi and Cahill, W. F. Exponential Integral and Related Functions. Handbook of Mathematical Functions, M. Abramowitz and I. A. Stegun, Ed., 10th Reprint., Dover Publications, pp 227-232 (1972).

[4] George Box, J. Stuart Hunter, and William G. Hunter. Statistics for Experimenters. Wiley-Interscience, Second Edition (May 1, 2005).

[5] Mark J. Kiemele, Stephen R. Schmidt, and Ronald J. Berdine. Basic Statistics: Tools for Continuous Improvement. Air Academy Press, Fourth Edition (January 1, 1997).

[6] Douglas C. Montgomery, George C. Hunger, and Norma F. Hubele. Engineering Statistics. John Wiley & Sons; 5th edition (December 21, 2010).

[7] Murray R. Spiegel and Larry J. Stephens. Schaum's Outline of Statistics. McGraw Hill, Sixth Edition (October 26, 2017).

[8] Multiple responses: The desirability approach. NIST Engineering Statistics Handbook, 5.5.3.2.2, National Institute of Standards and Technology at the U.S. Department of Commerce.